

## AGB yields and Galactic Chemical Evolution: last updated

This content has been downloaded from IOPscience. Please scroll down to see the full text.

2016 J. Phys.: Conf. Ser. 665 012023

(<http://iopscience.iop.org/1742-6596/665/1/012023>)

View [the table of contents for this issue](#), or go to the [journal homepage](#) for more

Download details:

IP Address: 129.13.72.197

This content was downloaded on 09/08/2017 at 07:15

Please note that [terms and conditions apply](#).

You may also be interested in:

### EVOLUTION OF FLUORINE IN THE GALAXY WITH THE $\nu$ -PROCESS

Chiaki Kobayashi, Natsuko Izutani, Amanda I. Karakas et al.

### Stellar Abundance and Galactic Chemical Evolution through LAMOST Spectroscopic Survey

Gang Zhao, Yu-Qin Chen, Jian-Rong Shi et al.

### GALACTIC CHEMICAL EVOLUTION: THE IMPACT OF THE $^{13}\text{C}$ -POCKET STRUCTURE ON THE $s$ -PROCESS DISTRIBUTION

Wiescher et al.

### ON THE NEED OF THE LIGHT ELEMENTS PRIMARY PROCESS (LEPP)

S. Cristallo, C. Abia, O. Straniero et al.

### Nitrogen Abundances and the Distance Moduli of the Pleiades and Hyades

Blake Miller, Jeremy R. King, Yu Chen et al.

### GALACTIC CHEMICAL EVOLUTION AND SOLAR $s$ -PROCESS ABUNDANCES: DEPENDENCE ON THE $^{13}\text{C}$ -POCKET STRUCTURE

R. Gallino et al.

### CARBON IN RED GIANTS IN GLOBULAR CLUSTERS AND DWARF SPHEROIDAL GALAXIES

Evan N. Kirby, Michelle Guo, Andrew J. Zhang et al.

### Fine-Structure Constant in Damped Ly Systems

Timothy P. Ashenfelder, Grant J. Mathews and Keith A. Olive

### CHEMICAL EVOLUTION LIBRARY FOR GALAXY FORMATION SIMULATION

Takayuki R. Saitoh

# AGB yields and Galactic Chemical Evolution: last updated

S Bisterzo<sup>1,2</sup>, C Travaglio<sup>2</sup>, M Wiescher<sup>3</sup>, R Gallino<sup>1</sup>, F Käppeler<sup>4</sup>, O Straniero<sup>5</sup>, S Cristallo<sup>5</sup>, G Imbriani<sup>6</sup>, J Görres<sup>3</sup> and R J deBoer<sup>3</sup>

<sup>1</sup> Department of Physics, University of Turin, Italy

<sup>2</sup> INAF - Astrophysical Observatory of Turin, Italy

<sup>3</sup> Department of Physics, University of Notre Dame, Notre Dame, IN

<sup>4</sup> Karlsruhe Institute of Technology, Karlsruhe, Germany

<sup>5</sup> Osservatorio Astronomico di Collurania, Teramo, Italy

<sup>6</sup> Dipartimento di Scienze Fisiche, Università di Napoli Federico II, Italy

E-mail: [bisterzo@to.infn.it](mailto:bisterzo@to.infn.it), [sarabisterzo@gmail.com](mailto:sarabisterzo@gmail.com)

**Abstract.** We study the *s*-process abundances at the epoch of the Solar-system formation as the outcome of nucleosynthesis occurring in AGB stars of various masses and metallicities. The calculations have been performed with the Galactic chemical evolution (GCE) model presented by [1, 2]. With respect to previous works, we used updated solar meteoritic abundances, a neutron capture cross section network that includes the most recent measurements, and we implemented the *s*-process yields with an extended range of AGB initial masses. The new set of AGB yields includes a new evaluation of the  $^{22}\text{Ne}(\alpha, n)^{25}\text{Mg}$  rate, which takes into account the most recent experimental information.

## 1. Introduction

The understanding of the *s*-process contribution to the isotopic abundances of heavy elements in the Solar System is fundamental to disentangle between several nucleosynthesis processes that have competed during the evolution of the Milky Way. The *s*-process abundances observed in the Solar System are the result of a complex Galactic chemical evolution process, which mainly accounts for the pollution of several AGB generations with different initial masses and metallicities.

It was shown that AGB stars with low initial masses ( $M = 1.5$  and  $3 M_{\odot}$ ), half solar metallicity, and a specific  $^{13}\text{C}$ -pocket choice (called case ST) reproduce the *main* component of the *s*-process [3], which synthesized about half of the elements from Sr to Pb. This approximation still provides strong information about the *s*-process contribution to isotopes in the region between  $^{134}\text{Ba}$  and  $^{204}\text{Pb}$  (see discussion in [4]).

Two additional *s*-process components should be considered to reproduce the solar abundances of light neutron capture isotopes up to Sr (the *weak* – *s* component) and the stable isotopes at the termination point of the *s*-path,  $^{208}\text{Pb}$  and  $^{209}\text{Bi}$  (the *strong* – *s* component). The *weak* – *s* process occurs in massive stars during core He and shell C burning and partly produces neutron capture isotopes lighter than  $A \sim 90$  ( $^{86,87}\text{Sr} \sim 10\%$ ; lower contribution to Y and Zr isotopes; see e.g., [5]). AGB stars with low metallicity and low initial mass synthesize about half of solar  $^{208}\text{Pb}$ , the so called *strong* – *s* component (see [6, 7]). The  $^{13}\text{C}$  in the pocket is primary, which



means it is directly synthesized in the star independently of the initial composition. Therefore, by decreasing the metallicity, the number of free neutrons per iron seed becomes so large to overcome the first and the second *s*-peaks (Sr-Y-Zr and Ba-La-Ce, respectively), to feed directly  $^{208}\text{Pb}$  (and  $^{209}\text{Bi}$ ).

Actually, the understanding of the origin of light *s*-process isotopes Sr, Y and Zr is more enigmatic. GCE models by [2] found that AGB yields underestimate the solar abundance of Sr, Y, Zr, and the solar composition of isotopes from  $^{86}\text{Sr}$  to  $^{130}\text{Xe}$  by about 20–30% (including the *s*-only  $^{96}\text{Mo}$ ,  $^{100}\text{Ru}$ ,  $^{104}\text{Pd}$ ,  $^{110}\text{Cd}$ ,  $^{116}\text{Sn}$ ,  $^{122,123,124}\text{Te}$  and  $^{130}\text{Xe}$ ). The *weak* – *s* process can not compensate the missing solar abundance, because it mainly produces isotopes up to Sr, with a negligible contribution up to  $^{130}\text{Xe}$ . Spectroscopic observations of peculiar metal-poor stars showing large enhancement in *r*-process elements<sup>1</sup> suggest that  $\sim 10\%$  of solar Sr-Y-Zr is due to the *r*-process. However, both *s*- and *r*-processes are not sufficient to explain the solar observations of light neutron capture elements. [2] hypothesized the existence of an additional process of unknown origin, called by the authors LEPP (light element primary process since it was supposed to be of primary origin). Several scenarios have been recently explored, both involving the secondary *s*-process in massive stars (e.g., *cs*-component by [9], which may explain the missing *s*-process component) or primary *r*-process during the advanced phases of explosive nucleosynthesis (see review [10], which may account of complementary *r*-contributions). Therefore, even if promising theoretical improvements related to the explosive phases of massive stars and core collapse Supernovae, as well as recent spectroscopic investigations [11, 12] have been made, a fully understanding about the origin of the neutron capture elements from Sr up to Xe is still lacking.

We aim to investigate the effects of a new set of AGB yields (with updated nuclear cross section network and solar abundances) on the solar *s*-process composition (Section 2).

## 2. Results

We focus the analysis on the variations of the Solar-system *s*-process GCE predictions by adopting updated AGB yields, and by testing the effects of different prescriptions on nuclear cross sections. The Galactic evolution is computed as function of time up to the present epoch ( $t_{\text{Today}} = 13.73 \pm 0.12$  by WMAP), following the three zones of the Galaxy, halo, thick and thin disk. We adopted the yields by [13] and [14] for SNe II and Ia, respectively.

Major revisions involve the solar system meteoritic abundances by [15], a neutron capture cross section network with the most recent published measurements, as well as a larger set of AGB yields that extend toward lower initial mass (down to  $M = 1.3 M_{\odot}$ ). We started from the AGB models presented by [16], which were based on the FRANEC code by [17, 18, 19].

A series of thousands of new AGB models have been run, for a total of 28 metallicities from  $[\text{Fe}/\text{H}] = +0.2$  down to  $-3.6$  (most of them focused on the metallicity range between solar and  $[\text{Fe}/\text{H}] = -1.6$ , where the isotopes of the three *s*-peaks are largely produced, see [1, 7, 2, 20]). Yields of a set of five AGB models with low initial masses ( $M = 1.3, 1.4, 1.5, 2,$  and  $3 M_{\odot}$ ) and two AGB models with intermediate initial masses ( $M = 5$  and  $7 M_{\odot}$ ) have been interpolated/extrapolated over the whole metallicity and mass range (hereafter LMS refers to the mass range between  $1.3 \leq M/M_{\odot} < 4$ , and IMS to  $4 \leq M/M_{\odot} < 8$ ). This assures a sufficiently high accuracy in the AGB mass and metallicity ranges.

Particularly challenging for the *s*-process is the understanding of the formation of the  $^{13}\text{C}$ -pocket, specifically the mass fraction of  $^{13}\text{C}$  and  $^{14}\text{N}$  in the pocket and the mass involved. Both uncertainties largely affect the *s*-yields (see e.g., [21, 22]). Current full evolutionary AGB models still adopt a free parametrization to reproduce the  $^{13}\text{C}$ -pocket, by means of overshooting

<sup>1</sup> E.g., CS 22892–052 and CS 31081–001 (see review by [8]), where the *rapid* neutron capture process is ascribed to explosive nucleosynthesis phases of massive stars.

(e.g., [23, 24, 25]) or other better physically justified prescriptions (e.g., new FRUITY models by [26, 27], and references therein; or mixing produced by magnetic fields, [28]). As suggested by the  $s$ -process spread observed at a given metallicity in different stellar populations (e.g., post-AGB, Ba, CH and CEMP- $s$  stars; [8, 29]), a range of the  $s$ -process efficiency strengths is needed. The theoretical reason of this spread observed among  $s$ -elements is still under investigation (AGB initial mass, magnetic fields, gravitational waves, or rotation, see [30]).

As discussed by [16], we artificially introduce the  $^{13}\text{C}$ -pocket in our post-process AGB calculations, and we treated it as a free parameter kept constant pulse by pulse. Starting from the  $^{13}\text{C}$ -pocket ST case, similar to that adopted by [6], we multiply or divide the  $^{13}\text{C}$  (and  $^{14}\text{N}$ ) abundances in the pocket by different factors. We considered an accurate weighted average of the  $^{13}\text{C}$ -pocket efficiencies in order to reproduce  $\sim 100\%$  of solar  $^{150}\text{Sm}$  and the other  $s$ -only isotopes heavier than  $A \sim 90$ . Note that  $^{150}\text{Sm}$  has well defined solar abundance, and it is the  $s$ -only isotope less affected by branchings and nuclear cross section uncertainties as well. A second reaction, the  $^{22}\text{Ne}(\alpha, n)^{25}\text{Mg}$ , starts to partially burn at  $T_8 = 3$  during thermal pulses and produces an efficient neutron burst mainly affecting isotopes close to the branching points.

Results are shown in Figure 1. The  $s$ -only isotopes are indicated by solid circles. Different symbols have been used for isotopes that receive additional contributions:  $^{128}\text{Xe}$ ,  $^{152}\text{Gd}$ , and  $^{164}\text{Er}$  (open squares), which have a non-negligible  $p$  contribution;  $^{176}\text{Lu}$  (open triangle), a long-lived isotope ( $3.8 \times 10^{10}$  yr), which decays into  $^{176}\text{Hf}$ ;  $^{187}\text{Os}$  (open triangle), which is affected by the long-lived decay of  $^{187}\text{Re}$  ( $4.1 \times 10^{10}$  yr);  $^{180}\text{Ta}$  (open circle), which also receives contributions from the  $p$  process and from  $\nu$ -nucleus interactions in massive stars;  $^{208}\text{Pb}$  (filled big square), half of which is produced by the strong- $s$  component. We compare the  $s$ -process predictions, calculated with the GCE model at the epoch of the Solar System formation ( $t_{\odot} = 9.17$  Gyr from the beginning of the birth of the Universe), with the meteoritic abundances by [15]. As shown in the *top panel*, LMS (black symbols) reproduce almost all the Solar System  $s$ -only isotopes between  $A = 140$  and 210. An additional small contribution ( $< 10\%$ ) comes from IMS for isotopes with  $A < 140$ . The total  $s$ -percentages (LMS + IMS) is represented by blue symbols. IMS AGBs play a minor role in the Galactic enrichment, because their He-intershell is smaller than in LMS by one order of magnitude, with an uncertain formation of the  $^{13}\text{C}$ -pocket and a less efficient third dredge-up. The  $^{22}\text{Ne}(\alpha, n)^{25}\text{Mg}$  neutron source is efficiently activated in IMS due to the high temperature reached at the bottom of the thermal pulses ( $T_8 = 3.5$ ). The peak neutron density reached in IMS easily allows a strong overproduction of  $^{86}\text{Kr}$ ,  $^{87}\text{Rb}$ , and  $^{96}\text{Zr}$ , three neutron rich isotopes affected by the branchings at  $^{85}\text{Kr}$  and  $^{95}\text{Zr}$ , which are very sensitive to the neutron density.

Particularly large is the abundance of  $^{96}\text{Zr}$  (big asterisk). Note that  $^{96}\text{Zr}$  is strongly sensitive to the number of thermal pulses experienced by the AGB models, as well as to the  $^{22}\text{Ne}(\alpha, n)^{25}\text{Mg}$  rate adopted. In general, an over-prediction of  $^{96}\text{Zr}$  may suggest a low number of thermal pulses for IMS. As discussed by [16], we assume a strong mass loss for IMS, which allows a total of 24 thermal pulses. Under this hypothesis, IMS produce about 30% of solar  $^{96}\text{Zr}$ , while an additional 70% comes from LMS (Figure 1, *top panel*).  $^{96}\text{Zr}$  is the most neutron rich stable Zr isotope, and a contribution of 100% from AGB is surely overestimated. Moreover, it disagrees with recent  $p$ -process predictions by [32], which estimate an additional non-negligible contribution to  $^{96}\text{Zr}$  by SNIa (up to 30%).

As a further improvement, we computed a new set of AGB yields that includes a new evaluation of the  $^{22}\text{Ne}(\alpha, n)^{25}\text{Mg}$  rate, which takes into account the most recent experimental information. The recommended value we are suggesting is very close to [34] and agrees with the recent determination of [35]. At AGB temperature ( $T_8 \sim 2.5$  to 3.5) the new  $^{22}\text{Ne}(\alpha, n)^{25}\text{Mg}$  rate is about a factor of 2 lower than our rate used so far (corresponding to the lower limit suggested by [36]<sup>2</sup>). The related new Solar-system abundances are displayed in Figure 1, *bottom*

<sup>2</sup> Note that we modified accordingly the rate of the  $^{22}\text{Ne}(\alpha, \gamma)^{26}\text{Mg}$ . Specifically, at the temperature of interest

panel, red symbols. As expected, major differences are shown close to the branchings points. In particular,  $\sim 50\%$  of solar  $^{96}\text{Zr}$  is produced by AGBs, in better agreement with expectations.

Updated GCE calculations plausibly reproduce within the uncertainties all  $s$ -only isotopes with  $A > 130$ , and confirm the missing 20% Solar  $s$ -contribution of  $s$ -only isotopic abundances between  $A = 96 - 130$  found by [2]. Variations with respect to the results presented by [29], their Fig. 15, bottom panel) are mainly due to new solar abundances, recent neutron capture cross section measurements, and the new evaluation of the  $^{22}\text{Ne}(\alpha, n)^{25}\text{Mg}$  rate.

Note that  $^{192}\text{Pt}$  and  $^{198}\text{Hg}$  are affected by large uncertainties: concerning  $^{192}\text{Pt}$ , the neutron capture cross section of  $^{191}\text{Os}$  and  $^{192}\text{Ir}$  evaluated theoretically at 22%, the extrapolation of the  $^{192}\text{Ir}$  measurement in stellar conditions (see discussion by [37], as well as the old measurement of the  $^{192}\text{Pt}(n, \gamma)$  reaction, with 20% of uncertainty at 30 keV [38]; moreover, Hg is too volatile for a reliable experimental determination of the solar abundance ([15] estimated an uncertainty of 20%).  $^{204}\text{Pb}$  (and all Pb isotopes) have well determined neutron capture cross sections (see [39]), but it is strongly affected by the branching at  $^{204}\text{Tl}$ , with variations of  $\sim 10\%$ .

Updated Solar  $s$ -process abundances of some selected elements are compared with previous GCE computations [7, 2] in Table 1. Marginal differences ( $< 5\%$ ) are seen in general. La and Ce are among the few exceptions: the larger  $s$ -contribution obtained by this work (+12% and +6%) is the consequence of the new  $^{139}\text{La}(n, \gamma)^{140}\text{La}$  rate measured by [40]. A more detailed comparison and a discussion concerning the most relevant updated information will be provided in a future work.

**Table 1.** The  $s$ -process contribution from LMS and IMS AGBs at the epoch of the Solar System formation (in percentages). Results by [7, 2] in column 2 are compared with updated results (this work, column 3), computed with all recently updated information, including the new  $^{22}\text{Ne}(\alpha, n)^{25}\text{Mg}$  rate. The  $r$ -process contribution (evaluated with the residual method  $N_r = N_s - N_\odot$ ) is given in column 4 (in percentages).

Element	s(2001-2004)	s(This work)	r(This work)
Sr	71	67	—
Y	69	70	—
Zr	65	64	—
Ba	80	83	17
La	61	73	27
Ce	75	81	19
Pr	47	49	51
Nd	54	56	44
Sm	30	31	69
Eu	6	6	94
Pb	91	88	12

## Acknowledgments

S.B. wishing to acknowledge JINA for financial support under ND Fund #201387 and 305387.

## References

- [1] Travaglio, C., Galli, D., Gallino, R., Busso, M., Ferrini, F., Straniero, O. 1999, ApJ, 521, 691
- [2] Travaglio, C., Gallino, R., Arnone, E., Cowan, J., Jordan, F., Sneden, C. 2004, ApJ, 601, 864

of AGBs, between  $T_8 = 2.5$  to 3.5, this rate is almost unchanged.

- [3] Arlandini, C., Käppeler, F., Wisshak, K., Gallino, R., Lugaro, M., Busso, M., Straniero, O. 1999, *ApJ*, 525, 886
- [4] Bisterzo, S., Gallino, R., Straniero, O., Cristallo, S., Käppeler F. 2011, *MNRAS*, 418, 284
- [5] Pignatari, M., Gallino, R., Heil, M., Wiescher, M., Käppeler, F., Herwig, F., Bisterzo, S. 2010, *ApJ*, 710, 1557
- [6] Gallino, R., Arlandini, C., Busso, M., Lugaro, M., Travaglio, C., Straniero, O., Chieffi, A., Limongi, M. 1998, *ApJ*, 497, 388
- [7] Travaglio, C., Gallino, R., Busso, M., Gratton, R. 2001, *ApJ*, 549, 346
- [8] Sneden, C., Cowan, J. J., Gallino, R. 2008, *ARA&A*, 46, 241
- [9] Pignatari, M., Hirschi, R., Wiescher, M., et al. 2013, *ApJ*, 762, 31
- [10] Thielemann, F.-K., Arcones, A., Käppeli, R., et al. 2011, *Progress in Particle and Nuclear Physics* 66, 346
- [11] Roederer I. U. 2012, *ApJ*, 756, 36
- [12] Hansen, C. J., Primas, F., Hartman, H., et al. 2012, *A&A*, 545, 31
- [13] Rauscher, T., Heger, A., Hoffman, R.D., & Woosley, S.E. 2002, *ApJ*, 576, 323
- [14] Travaglio, C., Hillebrandt, W., Reinecke, M., & Thielemann, F.-K. 2004b, *A&A*, 425, 1029
- [15] Lodders, K., Palme, H., Gail, H.-P. 2009, in Trümper J. E., ed., *Landolt- Börnstein Group VI Astronomy and Astrophysics Numerical Data and Functional Relationships in Science and Technology, 4B: Solar System, 4.4*. Springer-Verlag, Berlin (doi:10.1007/978-3-540-88055-4-34)
- [16] Bisterzo, S., Gallino, R., Straniero, O., Cristallo, S., Käppeler F. 2010, *MNRAS*, 404, 1529
- [17] Straniero, O., Gallino, R., Busso, M., Chieffi, A., Raiteri, C. M., Limongi, M., Salaris, M. 1995, *ApJ*, 440, L85
- [18] Straniero, O., Limongi, M., Chieffi, A., Domínguez, I., Busso, M., Gallino, R. 2000, *Mem. Soc. Astron. Ital.*, 71, 719
- [19] Straniero, O., Domínguez, I., Cristallo, S., Gallino, R. 2003, *PASA*, 20, 389
- [20] Serminato A., Gallino R., Travaglio C., Bisterzo S., Straniero O., *PASA*, 26, 153
- [21] Straniero, O., Gallino, R., Cristallo, S. 2006, *Nucl. Phys. A*, 777, 311
- [22] Herwig, F. 2005, *Annu. Rev. Astron. Astrophys.*, 43, 435
- [23] Herwig, F. 2000, *Astron. Astrophys.* 360, 952968
- [24] Herwig, F., Pignatari, M., Woodward, P. R., et al. 2011, *ApJ*, 727, 89
- [25] Karakas, A. I. 2010, *MNRAS*, 403, 1413
- [26] Cristallo, S., Straniero, O., Gallino, R., Piersanti, L., Domínguez, I., Lederer, M. T. 2009, *ApJ*, 696, 797
- [27] Cristallo, S., Piersanti, L., Straniero, O., et al. 2011, *ApJS*, 197, 17
- [28] Busso, M., Palmerini, S., Maiorca, E., Trippella, O., Magrini, L., Randich, S. 2012, 12th Symposium on Nuclei in the Cosmos, August 5 - 12, Cairns, Australia, 20
- [29] Käppeler, F., Gallino, R., Bisterzo, S., Aoki, W., 2011, *Rev. Mod. Phys.*, 83, 157
- [30] Piersanti, L., Cristallo, S., & Straniero, O. 2013, *ApJ*, 774, 98
- [31] Bisterzo, S., Gallino, R., Käppeler, F., et al. 2015, *MNRAS*, 449, 506
- [32] Travaglio, C., Röpke, F. K., Gallino, R., Hillebrandt, W., 2011, *ApJ*, 739, 93
- [33] Winckler, N., Dababneh, S., Heil, M., et al. 2006, *ApJ*, 647, 685
- [34] Jaeger, M., Kunz, R., Mayer, A., Hammer, J. W., Staudt, G., Kratz, K. L., Pfeiffer, B. 2001, *Phys. Rev. Lett.*, 87, 202501,
- [35] Longland, R., Iliadis, C., & Karakas, A. I. 2012, *Phys. Rev. C*, 85, 065809
- [36] Käppeler, F., Wiescher, M., Giesen, U., et al. 1994, *ApJ*, 437, 396
- [37] Rauscher, T. 2012, *ApJL*, 755,10
- [38] Bao, Z. Y., Beer, H., Käppeler F., Voss, F., Wisshak, K. 2000, *Atomic Data & Nuclear Data Tables*, 76, 70
- [39] KADoNiS v0.3, Karlsruhe Astrophysical Data Base of Nucleosynthesis in Stars, web site <http://www.kadonis.org/>
- [40] Winckler, N., Dababneh, S., Heil, M., et al. 2006, *ApJ*, 647, 685

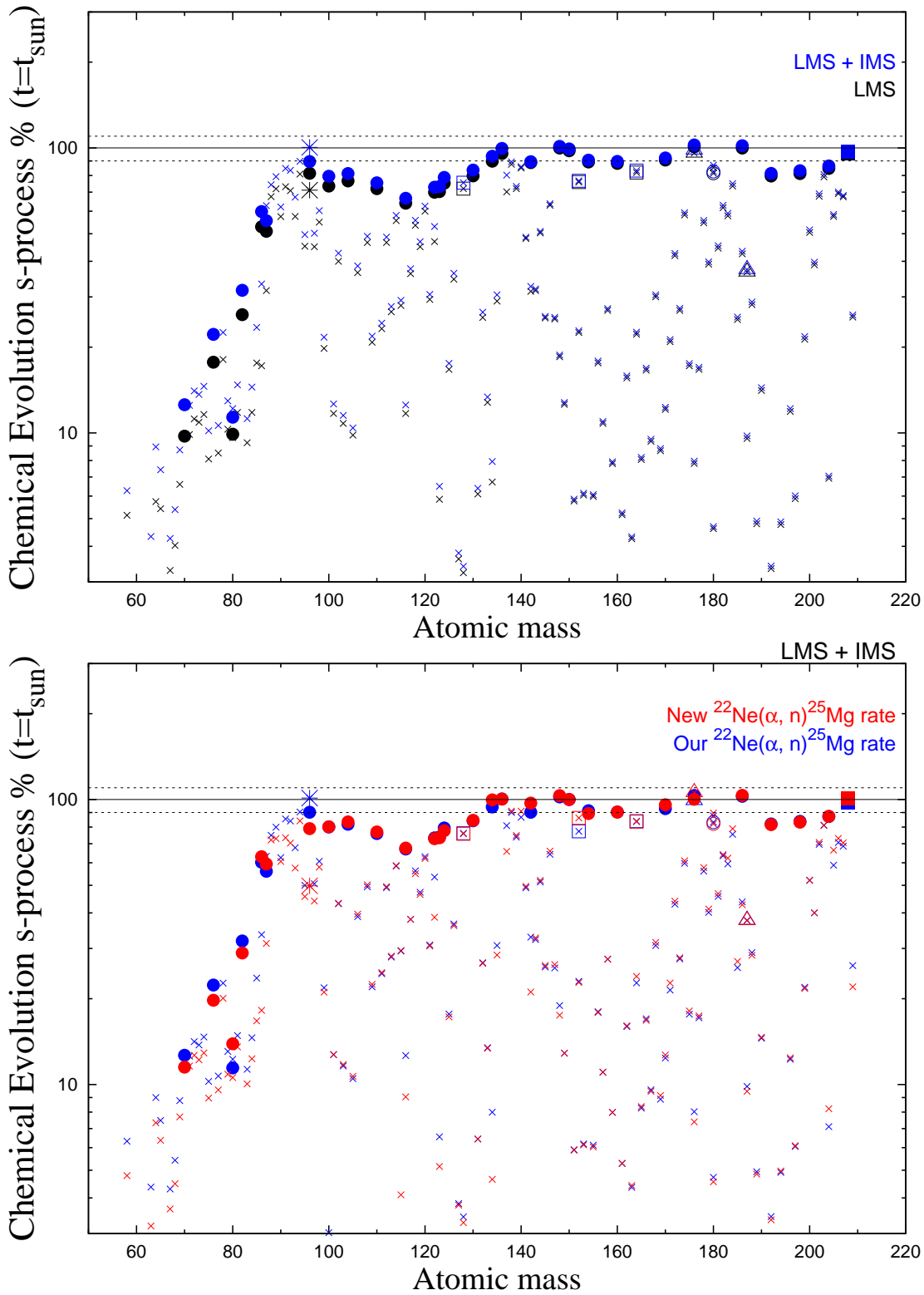


**Figure 1.** Reproduction of the Solar  $s$ -process abundances (in %) obtained at the epoch of the Solar System formation with GCE model. We used a neutron capture cross section network that includes the most recent measurements (see [31]) and we implemented the  $s$ -process yields with an extended range of AGB initial masses. Updated solar meteoritic abundances by [15] are adopted. The  $s$ -only isotopes are indicated by solid circles.  $^{96}\text{Zr}$  is represented by a big asterisk. Different symbols have been used for isotopes that receive additional contributions (see text). *Top panel:* we distinguish between the contribution of LMS alone (black symbols) and the total  $s$ -contribution of all AGB masses (LMS + IMS; blue symbols). *Bottom panel:* we display the total  $s$ -contribution shown in top panel (blue) in comparison to the results obtained with a new evaluation of the  $^{22}\text{Ne}(\alpha, n)^{25}\text{Mg}$  reaction (see text).